ISSN 1674-1056
http://cpb.iphy.ac.cn
http://iopscience.iop.org/cpb
中国物理 B
Chinese Physics
中国物理
Chinese Physics B

Hunting problems of multi-quadrotor systems via bearing-based hybrid protocols with hierarchical network

Zhen Xu(徐振), Xin-Zhi Liu(刘新芝), Qing-Wei Chen(陈庆伟), Zi-Xing Wu(吴梓杏)
Citation: Chin. Phys. B . 2020, 29(5): 050701 . **doi:** 10.1088/1674-1056/ab7da2
Journal homepage: http://cpb.iphy.ac.cn; http://iopscience.iop.org/cpb

What follows is a list of articles you may be interested in

Finite-time Mittag-Leffler synchronization of fractional-order delayed memristive neural networks with parameters uncertainty and discontinuous activation functions

Chong Chen(陈冲), Zhixia Ding(丁芝侠), Sai Li(李赛), Liheng Wang(王利恒)
Chin. Phys. B . 2020, 29(4): 040202 . **doi:** 10.1088/1674-1056/ab7803

Simulation of the influence of imperfections on dynamical decoupling of a superconducting qubit

Ying-Shan Zhang(张颖珊), Jian-She Liu(刘建设), Chang-Hao Zhao(赵昌昊), Yong-Cheng He(何永成), Da Xu(徐达), Wei Chen(陈炜)
Chin. Phys. B . 2019, 28(6): 060201 . **doi:** 10.1088/1674-1056/28/6/060201

H_∞ couple-group consensus of stochastic multi-agent systems with fixed and Markovian switching communication topologies

Muyun Fang(方木云), Cancan Zhou(周灿灿), Xin Huang(黄鑫), Xiao Li(李晓), Jianping Zhou(周建平)
Chin. Phys. B . 2019, 28(1): 010703 . **doi:** 10.1088/1674-1056/28/1/010703

Distance-based formation tracking control of multi-agent systems with double-integrator dynamics

Zixing Wu(吴梓杏), Jinsheng Sun(孙金生), Ximing Wang(王希铭)
Chin. Phys. B . 2018, 27(6): 060202 . **doi:** 10.1088/1674-1056/27/6/060202

Leader-following consensus of discrete-time fractional-order multi-agent systems

Erfan Shahamatkhah, Mohammad Tabatabaei
Chin. Phys. B . 2018, 27(1): 010701 . **doi:** 10.1088/1674-1056/27/1/010701

Hunting problems of multi-quadrotor systems via bearing-based hybrid protocols with hierarchical network*

Zhen Xu(徐振)[1,2], Xin-Zhi Liu(刘新芝)[2], Qing-Wei Chen(陈庆伟)[1,†], and Zi-Xing Wu(吴梓杏)[1,2]

[1] School of Automation, Nanjing University of Science and Technology, Nanjing 210094, China
[2] Department of Applied Mathematics, University of Waterloo, Waterloo N2L 3G1, Canada

(Received 21 January 2020; revised manuscript received 20 February 2020; accepted manuscript online 3 March 2020)

Bearing-based hunting protocols commonly adopt a leaderless consensus method, which requests an entire state of the target for each agent and ignores the necessity of collision avoidance. We investigate a hunting problem of multi-quadrotor systems with hybrid bearing protocols, where the quadrotor systems are divided into master and slave groups for reducing the onboard loads and collision avoidance. The masters obtain the entire state of the target, whose hybrid protocols are based on the displacement and bearing constraints to maintain formation and to avoid the collision in the hunting process. However, the slaves' protocols merely depend on the part state of the masters to reduce loads of data transmission. We also investigate the feasibility of receiving the bearing state from machine vision. The simulation results are given to illustrate the effectiveness of the proposed hybrid bearing protocols.

Keywords: hunting problem, multi-quadrotor system, bearing constraint, hierarchical network

PACS: 07.05.Dz, 02.30.Yy, 02.20.–a **DOI:** 10.1088/1674-1056/ab7da2

1. Introduction

Remote-controlled rotorcrafts and their formation tactics have received much attention in recent years due to their low cost, convenient operation and excellent maneuverability. The multi quadrotor systems play a preferred role in material transportation, forest fire fighting,[1] target tracking,[2] battlefield reconnaissance and strike,[3] mapping[4] and so forth. This paper focuses on performing the hunting task efficiently and reliably.

The hunting problem is a particular case of formation control containing a definite moving target. At present, the standard formation methods mainly classify as position-based control, displacement-based control and distance-based control, as shown in Figs. 1(a)–(c).

The position-based formation senses their positions in the global coordinate system without error feedback. It has derived a variety of straightforward methods in applications such as leader-follower[5] and virtual structure methods.[6] In the displacement-based protocol, each agent can sense the relative positions of its neighboring agents in the global coordinate system. Many displacement-based consensus protocols have been proposed to achieve consensus of a multi-agent system. In Ref. [7] a novel hybrid consensus protocol with dynamically changing interaction topologies was designed to take the time-delay into account. In Ref. [8] a new distributed protocol was presented to solve the mean square leader-following consensus problem for the nonlinear multi-agent systems, which contains a designed signal to dominate the effects of unmodeled dynamics. An adaptive finite-time control for the stochastic nonlinear systems driven by the noise of covariance was proposed in Ref. [9]. The distance-based control strategies requires less information than the others. The orientations of local coordinate systems in distance-based formation are not necessarily aligned with each other. Thus the trajectories may be different even if the initial values are equal (see e.g., Refs. [10,11]).

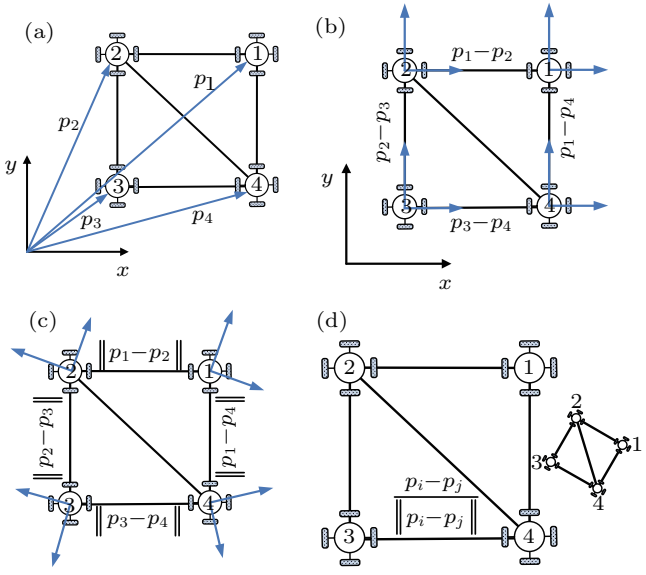


Fig. 1. Four kinds of the formation methods. (a) The position-based formation, (b) the displacement-based formation, (c) the distance-based formation, (d) the bearing-based formation.

These three methods apply to most consensus application scenarios associated with graph theory. However, they

*Project supported by the National Natural Science Foundation of China (Grant Nos. 61673217 and 61673214), the National Defense Basic Scientific Research Program of China (Grant No. JCKY2019606D001), and the China Scholarship Council.

†Corresponding author. E-mail: xz940706@163.com

© 2020 Chinese Physical Society and IOP Publishing Ltd

have difficulties to adjust the formation in the hunting process. The agents persist in reaching the desired position far fast, and the formation is chaotic and unorganized before convergence. If the target rush at the gap of the formation suddenly, the quadrotor systems would generate a high overshoot, which decreases the success rate of hunting.[12] To resolve the conflict between dynamic formation and the reliability of hunting, researchers presented a new bearing-based formation method for the first time in 2011.[13] This method drives the agents to circle the target with the same angular speed, which can prevent the target from escaping from the encirclement before convergence.

In Ref. [14] the bearing-based maneuver control of multi-agent formation to arbitrary dimensions was presented. In Ref. [15] two types of position estimation laws were combined with bearing-based protocols for improving the position accuracy. The modeling and controller design methods of first-order multi-agent systems are discussed systematically in Ref. [16]. In Ref. [17] an adaptive control law was designed based on the reference acceleration for networked thrust-propelled vehicles with parametric uncertainties. Even though the bearing-based formation method has made significant progress recently, dealing with the hunting scenarios based on the bearing state is still an open problem. The current achievements mainly focus on the single-integrator kinematic models, and the acquisition of bearing information is not mentioned. Meanwhile, the common bearing-based hunting protocols ignore the necessity of collision avoidance, and the formation converges to a point. Much more importantly, the hunting protocols request the entire state of the target for each agent, which aggravates loads of data transmission.

In this paper, we study the model of multi-quadrotor systems and propose a practical controller input of each quadrotor. The simulation approximates to the real situation, which improves the feasibility of engineering applications. Meanwhile, according to the research achievements in Ref. [18] we investigate the feasibility of receiving the bearing state by machine vision. In order to reduce the onboard loads and to ensure the safe distance of the quadrotor systems, we introduce a hierarchical network approach and design protocols for masters and slaves respectively. The masters are driven by the hybrid protocols based on both displacement error and bearing constraint, which act as skeleton and avoid the collision in the hunting process. Simultaneously, the slaves merely depend on the bearing states of adjacent masters to reduce loads of data transmission to maintain the formation. We illustrate that the bearing-based hybrid formation protocol is one of the most effective solutions to the hunting problem.

The outline of this paper is given as follows. In Section 2 we present some preliminaries and the acquisition of bearing information. In Section 3 we expound the principles and mission objectives of the hunting problem based on bearing control. In Sections 4 and 5, we provide the hybrid protocols of masters and slaves and analyze their convergence. In Section 6, we present the simulation test and analysis. Lastly, conclusions and future work are given in Section 7.

2. Preliminaries

2.1. Graph theory of MAS

Consider a multi-agent system with at least 2 masters. One can use a graph to describe the communication topology. Let $\mathcal{G} = (\mathcal{V}, \mathcal{E})$ be a directed graph with n nodes and h edges, where $\mathcal{V} = \{v_1, \ldots, v_n\}$ is the set of nodes and $\mathcal{E} \subset \mathcal{V} \times \mathcal{V}$ is the set of edges.

The incidence matrix $\boldsymbol{E}$ is defined as follows:

$$E_{ki} = \begin{cases} 1, & \text{if vertex } i \text{ is the head of edge } k, \\ -1, & \text{if vertex } i \text{ is the tail of edge } k, \\ 0, & \text{otherwise.} \end{cases} \tag{1}$$

The adjacency matrix $\boldsymbol{A}$ is defined as follows:

$$A_{ij} = \begin{cases} 1, & i \neq j, \quad j \in N_i, \\ 0, & i \neq j, \quad j \notin N_i. \end{cases} \tag{2}$$

Donate $1_n = [1, \ldots, 1]^T \in \mathbb{R}^n$ and $\boldsymbol{I}_d = \mathrm{diag}(1, \ldots, 1) \in \mathbb{R}^{d\times d}$. Here $\|\cdot\|$ represents the 2-norm for matrixes in $\mathbb{R}^{n\times n}$ or the Euclidean norm for vector in $\mathbb{R}^n$.

2.2. Theory of bearing constraint

Define a finite collection $\Xi = \{p_1, p_2, \ldots, p_n\} \in \mathbb{R}^n$ $(n \geq 2)$, in which p_i represents the coordinate position of node i. A configuration is denoted as $p = [p_1^{\mathrm{T}}, p_2^{\mathrm{T}}, \ldots, p_n^{\mathrm{T}}]^{\mathrm{T}} \in \mathbb{R}^{dn}$. A framework, denoted as $\mathcal{G}(p)$, is a combination containing the directed graph $\mathcal{G}$ and the configuration information of p. In the framework, only masters can obtain the position information p_{t} of the target, while the slaves merely depend on the bearing states of adjacent masters.

We define the framework between masters and slaves as

$$\zeta_{ij} \triangleq p_j - p_i, \xi_{ij} \triangleq \zeta_{ij}/\|\zeta_{ij}\|, \quad \forall (i,j) \in \mathcal{E}, \tag{3}$$

where ξ_{ij} represents the unit vector from p_j to p_i, which contains the bearing information, and $\xi_{ij} = -\xi_{ji}$.

Similarly, considering the target position, we can denote the framework between target and agents as

$$\zeta_{\mathrm{it}} \triangleq p_{\mathrm{t}} - p_i, \xi_{\mathrm{it}} \triangleq \zeta_{\mathrm{it}}/\|\zeta_{\mathrm{it}}\|, \quad \forall i \in \mathcal{V}, \tag{4}$$

and for a nonzero vector, we can define the projection operator $P(x) : \mathbb{R}^d \to \mathbb{R}^{d\times d}$ [16] as

$$\boldsymbol{P}(x) \triangleq \boldsymbol{I}_{\mathrm{d}} - \frac{x}{\|x\|}\frac{x^{\mathrm{T}}}{\|x\|}, \tag{5}$$

where $\boldsymbol{P}(x)$ can project any vector x onto its orthogonal complement. Note $\boldsymbol{P}(x)^{\mathrm{T}} = \boldsymbol{P}(x), \boldsymbol{P}(x)^2 = \boldsymbol{P}(x), \boldsymbol{P}(x) \geq 0$ and $\mathrm{Null}(\boldsymbol{P}(x)) = \mathrm{span}\{x\}$.[12] The projection operator can be

used to check whether two vectors in space are parallel or not. Therefore, we can obtain the following definitions.

Definition 1 (Bearing Congruency) For two graphs $\mathcal{G}(p)$ and $\mathcal{G}(p')$ with the same number of nodes, if any sides $\{\xi_{ij}, \xi'_{ij}\}$ between the nodes $\{p_i, p_j\} \in \mathcal{V}$, $\boldsymbol{P}(\xi_{ij}) \cdot (\xi'_{ij}) = 0$ are satisfied, $\mathcal{G}(p)$ and $\mathcal{G}(p')$ will be bearing congruency.

Here $\mathcal{G}(p')$ can be a different graph or a different moment in the same graph. When one obtains the relative bearing information between the agents without a global reference frame, the bearing function can be defined below.

Definition 2 (Bearing Function) Note that ζ_k and ξ_k are the vector and bearing of k-th edge respectively, then $\zeta_k = \zeta_{ij}, \xi_k = \xi_{ij}$, where $(i, j) \in \mathcal{E}$. Then the bearing function $\boldsymbol{F}_{\mathrm{B}} : \mathbb{R}^{dn} \to \mathbb{R}^{dh}$ can be defined as

$$\boldsymbol{F}_{\mathrm{B}}(p) \triangleq \left[\xi_1{}^{\mathrm{T}}, \ldots, \xi_k{}^{\mathrm{T}}, \ldots, \xi_h{}^{\mathrm{T}}\right]^{\mathrm{T}} \in \mathbb{R}^{dh}. \tag{6}$$

The jacobian matrix of the bearing function is defined as

$$\boldsymbol{R}_{\mathrm{B}}(p) \triangleq \frac{\partial \boldsymbol{F}_{\mathrm{B}}(p)}{\partial p}. \tag{7}$$

One can obtain the derivative of each bearing vector as

$$\frac{\partial \xi_k}{\partial \zeta_k} = \frac{1}{\|\zeta_k\|}\left(\boldsymbol{I}_{\mathrm{d}} - \frac{\zeta_k}{\|\zeta_k\|}\frac{\zeta_k{}^{\mathrm{T}}}{\|\zeta_k\|}\right) = \frac{1}{\|\zeta_k\|}\boldsymbol{P}_{\xi_k}, \tag{8}$$

where $\boldsymbol{P}_{\xi_k} = \boldsymbol{P}(\xi_k)$.

Considering $\zeta_k = (\boldsymbol{E} \otimes \boldsymbol{I}_d)p$ and $\xi_{ij} \triangleq p_{ij}/\|p_{ij}\|$.

$$\begin{aligned} \boldsymbol{R}_{\mathrm{B}} &= \frac{\partial \boldsymbol{F}_{\mathrm{B}}(p)}{\partial p} = \frac{\partial \boldsymbol{F}_{\mathrm{B}}(p)}{\partial \zeta_k}\frac{\partial \zeta_k}{\partial p} \\ &= \mathrm{diag}\left(\frac{\boldsymbol{P}_{\xi_k}}{\|\zeta_k\|}\right)(\boldsymbol{E} \otimes \boldsymbol{I}_{\mathrm{d}}). \end{aligned} \tag{9}$$

We will model the hunting problem accordingly.

2.3. Mathematical model of multi-quadrotor system

The quadrotor is an under-actuated system, and the coupling relationship between attitude angles and position is the core of modeling. According to the Euler–Lagrange modeling principle and the assumptions,[19] the dynamic model of the quadrotor is established as

$$\begin{aligned} &\dot{p}_i = V_i, \\ &m\dot{V}_i = U_{1i}\boldsymbol{R}e_3 - mge_3 + d_{\mathrm{F}}, \\ &\dot{\Theta}_i = \Omega_i, \\ &J\dot{\Omega}_i = \Gamma - \boldsymbol{C}\Omega_i + d_{\Gamma}, \end{aligned} \tag{10}$$

where $p_i = (x_i, y_i, z_i)^{\mathrm{T}}$ is the coordinate of the quadrotor in the inertial system; $\Theta_i = (\phi_i, \theta_i, \varphi_i)^{\mathrm{T}}$ is the attitude angle; m and g are mass and acceleration of gravity respectively; $e_3 = [0, 0, 1]^{\mathrm{T}}$ is the unit vector; $\boldsymbol{R} \in \mathbb{R}^{3\times3}$ is the translation relationship of velocity from the body coordinate system to the inertial coordinate system; $J\dot{\Omega}_i = (I_x\dot{\Omega}_{ix}, I_y\dot{\Omega}_{iy}, I_z\dot{\Omega}_{iz})^{\mathrm{T}}$ is the rotational inertia of quadrotor where Ω_i are the angular velocities of quadrotor attitude; Γ is controlling torque; $\boldsymbol{C} \in \mathbb{R}^{3\times3}$ represents coriolis force and centrifugal force; U_{1i} is the actual position control input for i-th quadrotor; d_{F} and $d_{\Gamma} \in \mathbb{R}^3$ are bounded disturbing terms.

In this dynamic model, the outer position loop drives the quadrotor toward the desired position with position controller U_{1i}, while the attitude inner loop tracks the desired angles. The attitude controller in the tracking problem was well established in Ref. [19], so we mainly focus on the design of the position controller in this paper.

Considering Eq. (10), we can rewrite the reduced equation of position loop as

$$\dot{p}_i = v_i, \quad \dot{v}_i = u_{p_i} + d_{\mathrm{F}}, \tag{11}$$

where $u_{p_i} = \frac{1}{m}U_{1i}\boldsymbol{R}e_3 - ge_3 \in \mathbb{R}^3$ is the virtual position controller of the i-th agent.

2.4. The meaning and acquisition of bearing state information

In this section, we briefly describe the way to obtain the bearing information in the engineering application.

According to Ref. [21], we can obtain the absolute position estimated by a combination of the monocular visual simultaneous localization and mapping (MVSLAM), and the air pressure sensor. MVSLAM provides the bearing information and the air pressure sensor provides an absolute scale respectively. However, considering the capability of data transmission, this approach only applies to a single quadrocopter. Another similar approach is to utilize artificial markers for simplifying position estimation. In Ref. [22], Scaramuzza and Fraundorfer proposed a system based on a low-cost commercial quadrotor with a monocular front-looking camera for performing autonomous hovering and waypoints following in an unknown environment.

The slaves aim to get the bearing information of the neighbor masters. In this process, the attitude angle $\varphi = 0$ for each quadrotor. Considering this simple requirement, we can utilize Engel's model and establish a three-dimensional coordinate system for the target in the field of camera view. The principle is shown in Fig. 2.

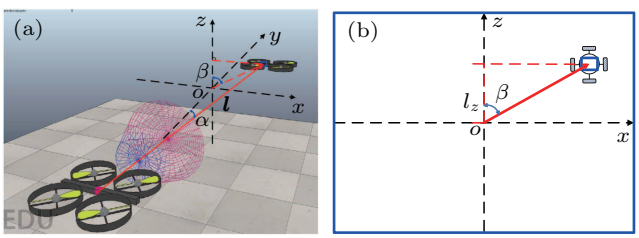


Fig. 2. The schematic of camera view. (a) The three-dimensional schematic, (b) the projection of schematic.

As shown in Fig. 2, $\boldsymbol{l}$ is the unit bearing vector from slave to master in cartesian coordinate, and the deviation angles (α,β) in Fig. 2(a) contain the bearing information. Here l_z is the projection of $\boldsymbol{l}$ on the z axis. The vertical component l_z is the height deviation between the slave and master on the camera view. If $l_z = 0$, the slave and master are on the same horizontal plane. It is easy to build a mapping between (α,β) and $\boldsymbol{l} = [x,y,z]$ so that we can calculate the current bearing from camera view immediately.

The spherical mapping $f(\alpha,\beta) : \mathbb{R}^2 \to \mathbb{R}^3$ is defined as

$$x = \sin\alpha\sin\beta, \quad y = \cos\alpha, \quad z = \sin\alpha\cos\beta. \tag{12}$$

It is noteworthy that the artificial markers should be easily distinguished and anti-disturbed, so conspicuous graphics or infrared markers are good choices. In this paper, we select eight highlighted yellow lights in two rows as an example, and the process of identification is shown in Fig. 3.

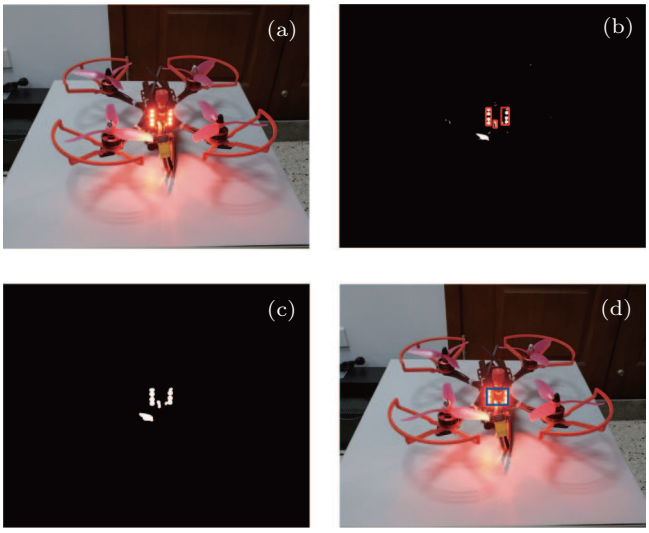


Fig. 3. The identification of markers: (a) the original image, (b) the identification of markers, (c) the filtering and corrosion, (d) the connected domain.

This method has a high demand for image quality and data transmission of a quadrotor. After the feature extraction and filtering of the image, we can construct the connected domain, which contains all the artificial markers. Somasundaram proposed remarkable spatiotemporal regions in Ref. [23] to extract the spatiotemporal features. Only a small percentage of the most salient (least self-similar) regions was considered and found using its algorithm, over which Spatio-temporal descriptors were computed.

3. Problem description

Figures 4 and 5 show the formation and principle of hunting comprising with n_m (≥ 2) masters and $n - n_m$ slaves. Consider the state of target T as (p_T, v_T, a_T). The control objective is to design a distributed control protocol for the multi-quadrotor system such that the quadrotors can construct an autonomous formation surrounding the target and gradually capture it.

To achieve obstacle avoidance in the hunting process, the master quadrotors have to collect the displacement information $D = [d_1, d_2, \ldots, d_{n_m}]^{\mathrm{T}}$ from the target and the following quadrotors only receive (or collect by cameras), where d_i is the displacement vector from the target to the i-th quadrotor. The formation spirally shrinks the hunting radius with rotated velocity $\omega_k(t)$ to prevent the target from escaping.

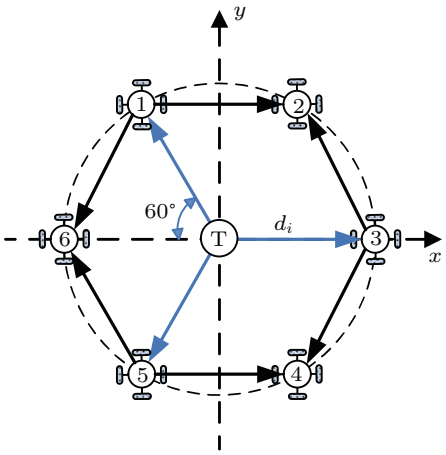


Fig. 4. The topology constructions between target and masters (blue lines), and between masters and slaves (black lines).

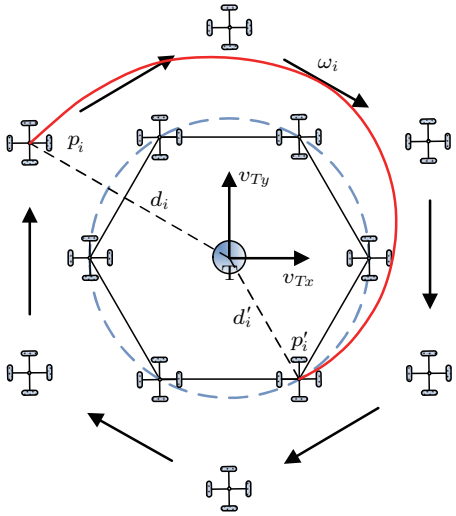


Fig. 5. Surrounding principle in xoy plane, where red line is the trajectory of i-th quadrotor.

To facilitate the understanding, the center and size of the multi-quadrotor system are defined as the evaluation functions.

Definition 3 (The center of multi-quadrotor)[16]

$$c(t) \triangleq \frac{1}{n}\sum_{i=1}^{n} p_i = \frac{1}{n}(1_n \otimes \boldsymbol{I}_{\mathrm{d}})^{\mathrm{T}} p. \tag{13}$$

Definition 4 (The formation size)[16]

$$s(t) = \sqrt{\frac{1}{n}\sum_{i=1}^{n} \|p_i - c(t)\|^2} = \frac{1}{\sqrt{n}} \|p - 1_n \otimes c(t)\|. \tag{14}$$

Definition 5 (The bearing Laplacian matrix) Matrix $\mathcal{L}_{\rm b}(\mathcal{G}) \in \mathbb{R}^{dn\times dn}$

$$[\mathcal{L}_{\rm b}(\mathcal{G})]_{ij} = \begin{cases} 0, & (i,j) \notin \mathcal{E}, \\ -\boldsymbol{P}(\xi_{ij}(t)), & (i,j) \in \mathcal{E}, \\ \sum\limits_{j\in N_i} \boldsymbol{P}(\xi_{ij}(t)), & i \in \mathcal{V}, \end{cases} \tag{15}$$

where $\mathcal{L}_{\rm b}(\mathcal{G})$ has the similar structure of the Laplacian matrix and contains the bearing information between the neighboring agents. According to the definition of the bearing Laplacian matrix, it can be expressed as

$$\mathcal{L}_{\rm b}(\mathcal{G}) = (\boldsymbol{E}\otimes \boldsymbol{I}_{\rm d})\,{\rm diag}(\boldsymbol{P}(\xi_k{}'))(\boldsymbol{E}^{\rm T}\otimes \boldsymbol{I}_{\rm d}). \tag{16}$$

Note that $\boldsymbol{P}(x)^{\rm T} = \boldsymbol{P}(x),\ \boldsymbol{P}(x)^2 = \boldsymbol{P}(x)$, so

$$\begin{aligned} \mathcal{L}_{\rm b}(\mathcal{G}) &= (\boldsymbol{E}\otimes \boldsymbol{I}_{\rm d}){\rm diag}(\boldsymbol{P}(\xi_k{}'))\,{\rm diag}(\boldsymbol{P}(\xi_k{}'))(\boldsymbol{E}^{\rm T}\otimes \boldsymbol{I}_{\rm d}) \\ &= \boldsymbol{R}_{\rm B}{}^{\rm T}\|\zeta_k\|\cdot\|\zeta_k\|\,\boldsymbol{R}_{\rm B} \\ &= \tilde{R}_{\rm B}^{\rm T}\tilde{R}_{\rm B}, \end{aligned} \tag{17}$$

where $\tilde{R}_{\rm B}^{\rm T} = \boldsymbol{R}_{\rm B}{}^{\rm T}\|\zeta_k\|$.

Meanwhile, $\mathcal{D}_{\rm b}(\mathcal{G}) \in \mathbb{R}^{dn_m\times dn_m}$ is the target bearing matrix, which represents the bearing information between the masters and the target,

$$[\mathcal{D}_{\rm b}(\mathcal{G})]_{ij} = \begin{cases} 0, & i \neq j, \\ P(\xi_{\rm it}(t)), & i = j, \end{cases} \tag{18}$$

where $\mathcal{D}_{\rm b}(\mathcal{G})$ and $\mathcal{L}_{\rm b}(\mathcal{G})$ are positive semi-definite matrixes.[12]

Considering the existence of the displacement vector, the general objective of hunting problem can be expressed as

$$\lim p_i - p_T = d_{i\rm d}, \tag{19}$$

where $d_{i\rm d}$ is the expected displacement of the i-th master.

The masters have already reserved vector constraints that contain formation and position information, while the displacement vectors of the slaves are difficultly obtained. Thus the objective can be rewritten with bearing information as

$$\begin{aligned} &\lim(p_m - 1_{n_m}\otimes p_T) = \boldsymbol{D}_{\rm d}, \\ &\xi_k(t) = \xi_k'(t) = \boldsymbol{R}(\omega^* t)\xi_k'(0)\boldsymbol{R}^{\rm T}(\omega^* t), \end{aligned} \tag{20}$$

where ω^* is the desired rotary velocity of the formation; $\boldsymbol{D}_{\rm d} = [d_{1\rm d},\ d_{2\rm d},\ldots,d_{n_m\rm d}]^{\rm T}$ is the desired displacement vector from the target to the masters; $\boldsymbol{R}(wt)$ is the rotation matrix in Eq. (10); $\xi_k'(t)$ is the desired bearing state of the edge k in t moment.

Note that if the slaves could keep the bearing structure, the displacement constraints will be satisfied sequentially. In general, the maximum cruising flight speed of commercial quadrotor $V_{\max} \approx 20$ m/s and the effective distance of protocols $l = 200$ m. Hence, one can consider bearing congruency under the condition of $\omega^*(t) \in [-0.1, 0.1]$ (rad/s) in this paper.[24]

4. Protocol design

In this section, to solve the hunting problem, distributed protocols for masters and slaves are designed respectively. First, we define the state for masters and slaves.

$$\begin{aligned} X_m &= k_a\mathcal{D}_{\rm b}\cdot{\rm sgn}(\boldsymbol{A})\otimes I_{\rm d}\cdot(\dot{p}_m - 1_{n_m}\otimes\dot{p}_T) \\ &\quad + k_b\cdot(\dot{p}_m - 1_{n_m}\otimes\dot{p}_T - \dot{\boldsymbol{D}}_{\rm d}), \\ X_s &= \mathcal{L}_{\rm b}(\mathcal{G})\cdot(k_\alpha p + k_\beta\dot{p}), \end{aligned} \tag{21}$$

where $\boldsymbol{A} = \left[\|p_1 - p_T\| - \|d_1\|,\ \ \|p_2 - p_T\| - \|d_2\|,\ \ \ldots,\ \|p_{n_m} - p_T\| - \|d_{n_m}\|\right]^{\rm T}$ is the master position constraint matrix; k_a, k_b, k_α and k_β are positive constants.

Then the controllers for masters and slaves are defined, respectively, as

$$\begin{aligned} u_{\rm pm} &= 1_{n_m}\otimes\ddot{p}_T - (p - 1_{n_m}\otimes p_T - \boldsymbol{D}_{\rm d}) - k_a\mathcal{D}_{\rm b}\cdot{\rm sgn}(\boldsymbol{A}) \\ &\quad \otimes I_{\rm d}(\dot{p}_m - 1_n\otimes\dot{p}_T) - k_b\cdot(\dot{p}_m - 1_{n_m}\otimes\dot{p}_T - \dot{\boldsymbol{D}}_{\rm d}) - \hat{d}_{\rm Fm}, \\ u_{\rm ps} &= -\mathcal{L}_{\rm b}(\mathcal{G})(k_\alpha p + k_\beta\cdot\dot{p}) - \hat{d}_{\rm Fs}, \end{aligned} \tag{22}$$

which can be rewritten as

$$\begin{aligned} u_{\rm pm} &= -X_m(t) + 1_{n_m}\otimes\ddot{p}_T - (p_m - 1_{n_m}\otimes p_T - \boldsymbol{D}_{\rm d}) - \hat{d}_{\rm Fm}, \\ u_{\rm ps} &= -X_s - \hat{d}_{\rm Fs}, \end{aligned} \tag{23}$$

where $\hat{d}_{\rm F} = [\hat{d}_{F1}^{\rm T}, \hat{d}_{F2}^{\rm T}, \ldots, \hat{d}_{Fn}^{\rm T}]^{\rm T}$ is the adaptive value of disturbance.

5. Hunting reliability analysis

5.1. The convergence of masters' displacement constraints

Theorem 1 Consider the system equation in Eq. (11), if the following conditions are satisfied: (i) $\omega_i{}^*(t) = \bar{\omega}_k \in [-0.1, 0.1]$ (rad/s) for all $i \in n - n_m$, (ii) the external disturbance $d_{\rm F}$ are bounded and slowly time-varying items where $\dot{d}_{\rm F} = 0$, then the multi-quadrotor system can hunt the target in accordance with the control protocols of Eq. (23).

Proof The position tracking error of masters can be defined as

$$z_1 = p_m - 1_{n_m}\otimes p_{\rm t} - \boldsymbol{D}_{\rm d}. \tag{24}$$

The derivative of error is

$$\dot{z}_1 = v_m - 1_{n_m}\otimes\dot{p}_{\rm t} - \dot{\boldsymbol{D}}_{\rm d}, \tag{25}$$

where $v_m = [v_1, v_2, \ldots, v_{n_m}]^{\rm T}$. Choose α as the expected positional velocity to approximate v,

$$\begin{aligned} \alpha &= 1_{n_m}\otimes\dot{p}_T - k_a{\rm sgn}(\boldsymbol{A})\otimes I_{\rm d}\cdot\mathcal{D}_{\rm b}(p_m - 1_{n_m}\otimes p_T) \\ &\quad - k_b\cdot(p_m - 1_n\otimes p_T - \boldsymbol{D}_{\rm d}), \end{aligned} \tag{26}$$

where α is an intermediate variable transformed from the first-order system control protocol.

Therefore, the tracking error of velocity in the second subsystem can be defined as

$$z_2 = v_m - \alpha. \tag{27}$$

The derivative of z_2 can be expressed as

$$\dot{z}_2 = u_{pm} + d_{\mathrm{F}m} - \dot{\alpha}. \tag{28}$$

The Lyapunov function of the system can be chosen as

$$V = \frac{1}{2} {z_1}^{\mathrm{T}} z_1 + \frac{1}{2} {z_2}^{\mathrm{T}} z_2 + \frac{1}{2\gamma_1} \tilde{d}_{\mathrm{F}m}^{\mathrm{T}} \tilde{d}_{\mathrm{F}m}, \tag{29}$$

where $\tilde{d}_{\mathrm{F}l} = d_{\mathrm{F}l} - \hat{d}_{\mathrm{F}l}$.

Using u_{pl} and the adaptive law $\dot{\tilde{d}}_{\mathrm{F}} = -\gamma_1 z_2$, the derivative of V_1 can be expressed as

$$\begin{aligned}
\dot{V}_1 &= {z_1}^{\mathrm{T}} \dot{z}_1 + {z_2}^{\mathrm{T}} \dot{z}_2 + \frac{1}{\gamma_1} \dot{\tilde{d}}_{\mathrm{F}m}^{\mathrm{T}} \tilde{d}_{\mathrm{F}m} \\
&= {z_1}^{\mathrm{T}} (v_m - \alpha + \alpha - 1_{n_m} \otimes \dot{p}_T) \\
&\quad + {z_2}^{\mathrm{T}} (u_{\mathrm{p}m} + d_{\mathrm{F}m} - \dot{\alpha}) + \frac{1}{\gamma_1} \dot{\tilde{d}}_{\mathrm{F}m}^{\mathrm{T}} \tilde{d}_{\mathrm{F}m} \\
&= {z_1}^{\mathrm{T}} z_2 + {z_1}^{\mathrm{T}} (-k_a \mathcal{D}_{\mathrm{b}} \cdot \mathrm{sgn}(\boldsymbol{A}) \otimes I_{\mathrm{d}} \cdot (p_m - 1_{n_m} \otimes p_T) \\
&\quad - k_b \cdot (p_m - 1_{n_m} \otimes p_T - \boldsymbol{D}_{\mathrm{d}})) \\
&\quad + {z_2}^{\mathrm{T}} (u_{\mathrm{p}m} + d_{\mathrm{F}m} - \dot{\alpha}) + \frac{1}{\gamma_1} \dot{\tilde{d}}_{\mathrm{F}m}^{\mathrm{T}} \tilde{d}_{\mathrm{F}m} \\
&= {z_1}^{\mathrm{T}} z_2 + {z_1}^{\mathrm{T}} (-k_a \mathcal{D}_{\mathrm{b}} \cdot \mathrm{sgn}(\boldsymbol{A}) \\
&\quad \otimes I_{\mathrm{d}} \cdot \frac{\| p_m - 1_{n_m} \otimes p_T \|}{\boldsymbol{A}} - k_b \cdot I_{d \times n_m}) z_1 \\
&\quad + {z_2}^{\mathrm{T}} (u_p + d_{\mathrm{F}m} - 1_{n_m} \otimes \ddot{p}_T - \ddot{\boldsymbol{D}}_{\mathrm{d}} \\
&\quad + k_a \mathcal{D}_{\mathrm{b}} \cdot \mathrm{sgn}(\boldsymbol{A}) \otimes I_{\mathrm{d}} (\dot{p}_m - 1_{n_m} \otimes \dot{p}_T) \\
&\quad + k_b \cdot (\dot{p}_m - 1_{n_m} \otimes \dot{p}_T - \dot{\boldsymbol{D}})) + \frac{1}{\gamma_1} \dot{\tilde{d}}_{\mathrm{F}m}^{\mathrm{T}} \tilde{d}_{\mathrm{F}m} \\
&= {z_1}^{\mathrm{T}} (-\boldsymbol{H}) z_1 + {z_2}^{\mathrm{T}} d_{\mathrm{F}} + \frac{1}{\gamma_1} \dot{\tilde{d}}_{\mathrm{F}m}^{\mathrm{T}} \tilde{d}_{\mathrm{F}m} \leq 0,
\end{aligned} \tag{30}$$

where $\boldsymbol{H}_l = -k_a \mathcal{D}_{\mathrm{b}} \cdot \mathrm{sgn}(A) \otimes I_{\mathrm{d}} \cdot \frac{\| p_m - 1_n \otimes p_T \|}{A} - k_b \cdot I_{d \times n_m} \leq \boldsymbol{0}$, $\dot{\alpha} = 1_{n_m} \otimes \ddot{p}_T - k_a D_b \cdot \mathrm{sgn}(A) \otimes I_{\mathrm{d}} (\dot{p}_m - 1_{n_m} \otimes \dot{p}_T) - k_b \cdot (\dot{p}_m - 1_{n_m} \otimes \dot{p}_T - \dot{D}_{\mathrm{d}})$.

According to LaSalle's invariance principle, except for the system equilibrium point, $V > 0$, $\dot{V} \leq 0$. Thus the hunting process is asymptotically stable, which means that the formation radius keeps decreasing until $p_m - 1_{n_m} \otimes p_{\mathrm{t}} = D_{\mathrm{d}}$. The proof of masters' convergence is complete.

5.2. The convergence of slaves' bearing constraints

Considering the bearing constraints of the slaves, we can define the bearing tracking error $z_3 \triangleq \sqrt{k_\alpha} \tilde{R}_{\mathrm{B}} \cdot p$. It can be transformed to

$$\begin{aligned}
z_3 &= \sqrt{k_\alpha} \tilde{R}_{\mathrm{B}} \cdot p \\
&= \sqrt{k_\alpha} \mathrm{diag}(\boldsymbol{P}(\xi_k{}')) (E^{\mathrm{T}} \otimes \boldsymbol{I}_{\mathrm{d}}) \cdot p \\
&= \sqrt{k_\alpha} \mathrm{diag}(\| \zeta_k \| \boldsymbol{P}(\xi_k{}')) \left[\frac{\zeta_1}{\| \zeta_1 \|}, \ldots, \frac{\zeta_h}{\| \zeta_h \|} \right] \\
&= \sqrt{k_\alpha} \mathrm{diag}(\| \zeta_k \|) \left[\boldsymbol{P}(\xi_1{}') \xi_1, \ldots, \boldsymbol{P}(\xi_h{}') \xi_h \right]^{\mathrm{T}},
\end{aligned} \tag{31}$$

When $z_3 \to \boldsymbol{0}$, $\boldsymbol{P}(\xi_k') \xi_k = 0$, i.e., $\xi_k(t) = \xi_k'(t)$.
The derivative of z_3 is

$$\dot{z}_3 = \sqrt{k_\alpha} \tilde{R}_{\mathrm{B}} \cdot v. \tag{32}$$

Choose β as expected bearing velocity to approximate v,

$$\beta = -k_\beta \mathcal{L}_{\mathrm{b}}(\mathcal{G}) \cdot p. \tag{33}$$

The tracking error of velocity in the second subsystem can be defined as

$$z_4 = v_s - \beta. \tag{34}$$

The derivative of z_2 can be expressed as

$$\dot{z}_4 = u_{ps} + d_{\mathrm{F}s} - \dot{\beta}. \tag{35}$$

The Lyapunov function of the system can be chosen as

$$V_2 = \frac{1}{2} {z_3}^{\mathrm{T}} z_3 + \frac{1}{2} {z_4}^{\mathrm{T}} z_4 + \frac{1}{2\gamma_2} \tilde{d}_{\mathrm{F}s}^{\mathrm{T}} \tilde{d}_{\mathrm{F}s} > 0, \tag{36}$$

where $\tilde{d}_{\mathrm{F}s} = d_{\mathrm{F}s} - \hat{d}_{\mathrm{F}s}$. Using the condition that $\mathcal{L}_{\mathrm{b}}(\mathcal{G}) = \tilde{R}_{\mathrm{B}}^{\mathrm{T}} \tilde{R}_{\mathrm{B}}$,

$$\begin{aligned}
\dot{V}_2 &= {z_3}^{\mathrm{T}} \dot{z}_3 + {z_4}^{\mathrm{T}} \dot{z}_4 + \frac{1}{\gamma_2} \tilde{d}_{\mathrm{F}s}^{\mathrm{T}} \dot{\tilde{d}}_{\mathrm{F}s} \\
&= {z_3}^{\mathrm{T}} \left(\sqrt{k_\alpha} \tilde{R}_b v \right) + {z_4}^{\mathrm{T}} \left(u_{\mathrm{p}s} + d_{\mathrm{F}s} - \dot{\beta} \right) + \frac{1}{\gamma_2} \tilde{d}_{\mathrm{F}s}^{\mathrm{T}} \dot{\tilde{d}}_{\mathrm{F}s} \\
&= \sqrt{k_\alpha} {z_3}^{\mathrm{T}} \tilde{R}_b (v_s - \beta + \beta) \\
&\quad + {z_4}^{\mathrm{T}} (u_{\mathrm{p}s} + d_{\mathrm{F}s} - \dot{\beta}) + \frac{1}{\gamma_2} \tilde{d}_{\mathrm{F}s}^{\mathrm{T}} \dot{\tilde{d}}_{\mathrm{F}s} \\
&= \sqrt{k_\alpha} {z_3}^{\mathrm{T}} \tilde{R}_b z_4 + {z_3}^{\mathrm{T}} \left(-\sqrt{k_\alpha} k_\beta \mathcal{L}_{\mathrm{b}}(\mathcal{G}) \right) z_3 + {z_4}^{\mathrm{T}} \\
&\quad \times \left(-k_\alpha \mathcal{L}_{\mathrm{b}}(\mathcal{G}) p - k_\beta \mathcal{L}_{\mathrm{b}}(\mathcal{G}) \dot{p} - \hat{d}_{\mathrm{F}s} + d_{\mathrm{F}s} + k_\beta \mathcal{L}_{\mathrm{b}}(\mathcal{G}) \dot{p} \right) \\
&\quad + \frac{1}{\gamma_2} \tilde{d}_{\mathrm{F}s}^{\mathrm{T}} \dot{\tilde{d}}_{\mathrm{F}s} \\
&= {z_3}^{\mathrm{T}} \left(-\sqrt{k_\alpha} k_\beta \mathcal{L}_{\mathrm{b}}(\mathcal{G}) \right) z_3 + {z_4}^{\mathrm{T}} d_{\mathrm{F}s} + \frac{1}{\gamma_2} \dot{\tilde{d}}_{\mathrm{F}s}^{\mathrm{T}} \tilde{d}_{\mathrm{F}s} \leq 0,
\end{aligned} \tag{37}$$

where $H_s = -\sqrt{k_\alpha} k_\beta \mathcal{L}_{\mathrm{b}}(\mathcal{G}) \leq 0$. Substitute Eq. (22) and $\dot{\tilde{d}}_{\mathrm{F}s} = -\gamma_2 z_4$ into $\dot{V}_2$, then $\dot{V}_2 = {z_3}^{\mathrm{T}} \left(-\sqrt{k_\alpha} k_\beta \mathcal{L}_{\mathrm{b}}(\mathcal{G}) \right) z_3 \leq 0$. The proofs of slaves' convergence and the bearing congruency are complete.

Remark 1 The static matrix inverse method cannot solve the time-varying matrix inverse, because of the parallel distribution of characteristics and the fitness of hardware implementation. Neural network, especially recursive neural network, can carry out real-time calculation. However, the computing capacity cannot be satisfied by the flight control board of UAV, so the approximate solution is obtained by means of transformation.

From the mathematical model of quadrotor systems in Eq. (10), one can obtain $U_1 \boldsymbol{R} e_3 = m u_{pi} + m g e_3$. However, we cannot calculate $\boldsymbol{R}^{-1}$ roughly.

Assume that $[U_x, U_y, U_z]^{\mathrm{T}} = U_1 \boldsymbol{R} e_3$ is another form of virtual control variables, then

$$\begin{bmatrix} U_x \\ U_y \\ U_z \end{bmatrix} = U_1 \boldsymbol{R} e_3 = U_1 \cdot \begin{bmatrix} C_\theta C_\varphi & S_\theta S_\phi C_\varphi - C_\phi S_\varphi & C_\phi S_\theta C_\varphi + S_\phi S_\varphi \\ C_\theta S_\varphi & S_\theta S_\phi S_\varphi + C_\phi C_\varphi & C_\phi S_\theta S_\varphi - S_\phi C_\varphi \\ -S_\theta & C_\theta S_\phi & C_\phi C_\theta \end{bmatrix} \begin{bmatrix} 0 \\ 0 \\ 1 \end{bmatrix}, \tag{38}$$

where C_x and S_x imply functions $\cos(x)$ and $\sin(x)$ respectively; $U_x = U_1(C_\phi S_\theta C_\varphi + S_\phi S_\varphi)$; $U_y = U_1(C_\phi S_\theta S_\varphi - S_\phi C_\varphi)$; $U_z = U_1 C_\phi C_\theta$.

Convert them to

$$\begin{bmatrix} U_x \\ U_y \end{bmatrix} = U_z \begin{bmatrix} C_\varphi & S_\varphi \\ S_\varphi & -C_\varphi \end{bmatrix} \begin{bmatrix} \tan\theta \\ \tan\phi \sec\theta \end{bmatrix}.$$

In order to obtain the attitude inner loop command signal, we multiply both sides by $[C_{\varphi_\mathrm{d}}, S_{\varphi_\mathrm{d}}]$ and $[S_{\varphi_\mathrm{d}}, -C_{\varphi_\mathrm{d}}]$, respectively. According to the range of $\theta_\mathrm{d}, \phi_\mathrm{d} \in (-\pi/2, \pi/2)$, one can calculate these values by arctan functions

$$\begin{aligned} \theta_\mathrm{d} &= \arctan\left(\frac{U_x C_{\varphi_\mathrm{d}} + U_y S_{\varphi_\mathrm{d}}}{U_z}\right), \\ \phi_\mathrm{d} &= \arctan\left(C_{\theta_\mathrm{d}} \frac{U_x S_{\varphi_\mathrm{d}} - U_y C_{\varphi_\mathrm{d}}}{U_z}\right). \end{aligned} \tag{39}$$

Then the actual control input can be expressed as

$$U_1 = \frac{U_z}{C_{\phi_\mathrm{d}} C_{\theta_\mathrm{d}}}. \tag{40}$$

Remark 2 It is worth noting that, due to the underactuated characteristics, quadrotor is impossible to track all 6 degrees of freedom. Thus tracking trajectory P and yaw angle φ is a reasonable control strategy, while keeping the other two euler angles stable and bounded. The intermediate instruction, θ_d and ϕ_d, is not a reference signal, but an instruction signal generated by the virtual control input to the attitude subsystem in order to track the reference position. The lift input in Eq. (40) is the actual control input.[19][20]

6. Simulations

In this section, an example is given to verify the effectiveness of the hunting protocol in the paper. MATLAB-R2017a is used to build the model and run the simulation. The initial parameters of all the quadrotors are shown in Table 1, where the disturbances $d_\mathrm{F} = 0.1 \cdot [\sin t, \cos t, \sin t \cdot \cos t]^\mathrm{T}$ for both masters and slaves. Choose a set of the protocol parameters $k_a = 0.5$, $k_b = 0.1$, $k_\alpha = 0.05$ and $k_\beta = 1$. The target moves with a constant velocity $v_T = [1,1,1]^\mathrm{T}$ from $[0,0,0]^\mathrm{T}$.

Table 1. Simulation parameters.

Variable	Parameter	Simulation value	Simulation value
I_x, I_y	rotational inertia	0.04	$\mathrm{kg \cdot m^2}$
I_z	rotational inertia	0.08	$\mathrm{kg \cdot m^2}$
m	mass	3	kg
K_{fa0}	air friction	0.05	$\mathrm{N \cdot s/m}$
K_{D0}	resistance coefficient	0.1	$\mathrm{N \cdot s/m}$
J_r	motor inertia	0.01	$\mathrm{kg.m^2}$
d_0	centroid distance	0.5	m
$\|\|d_i\|\|$	length of displacement	100	m

According to the topology in Fig. 3, the initially expected bearing constraints between agents are

$$\begin{aligned} p'_{12} &= -p'_{21} = [1,0,0]^\mathrm{T}, \\ p'_{23} &= -p'_{32} = [\frac{1}{2}, -\frac{\sqrt{3}}{2}, 0]^\mathrm{T}, \\ p'_{34} &= -p'_{43} = [-\frac{1}{2}, -\frac{\sqrt{3}}{2}, 0]^\mathrm{T}, \\ p'_{45} &= -p'_{54} = [-1,0,0]^\mathrm{T}, \\ p'_{56} &= -p'_{65} = [\frac{1}{2}, -\frac{\sqrt{3}}{2}, 0]^\mathrm{T}, \\ p'_{61} &= -p'_{16} = [\frac{1}{2}, \frac{\sqrt{3}}{2}, 0]^\mathrm{T}. \end{aligned} \tag{41}$$

Using the definition of projection operator in Eq. (5), we can work out

$$\begin{aligned} \boldsymbol{P}'_{12}(0) &= \boldsymbol{P}'_{45}(0) = \boldsymbol{P}'_{3t}(0) = \boldsymbol{P}'_{6t}(0) = \begin{bmatrix} 0 & 0 & 0 \\ 0 & 1 & 0 \\ 0 & 0 & 1 \end{bmatrix}, \\ \boldsymbol{P}'_{23}(0) &= \boldsymbol{P}'_{56}(0) = \boldsymbol{P}'_{1t}(0) = \boldsymbol{P}'_{4t}(0) = \begin{bmatrix} \frac{3}{4} & \frac{\sqrt{3}}{4} & 0 \\ \frac{\sqrt{3}}{4} & \frac{1}{4} & 0 \\ 0 & 0 & 1 \end{bmatrix}, \\ \boldsymbol{P}'_{34}(0) &= \boldsymbol{P}'_{61}(0) = \boldsymbol{P}'_{2t}(0) = \boldsymbol{P}'_{5t}(0) = \begin{bmatrix} \frac{3}{4} & -\frac{\sqrt{3}}{4} & 0 \\ -\frac{\sqrt{3}}{4} & \frac{1}{4} & 0 \\ 0 & 0 & 1 \end{bmatrix}, \\ \boldsymbol{P}'_{ij}(t) &= \boldsymbol{R}(\omega t) \boldsymbol{P}'_{ij}(0) \boldsymbol{R}(\omega t)^\mathrm{T}. \end{aligned} \tag{42}$$

Then, the hunting trajectory and its performance are shown as follows.

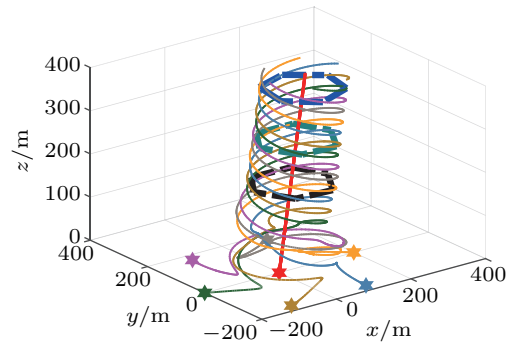


Fig. 6. The trajectory (full lines) and fragments (imaginary lines) of multi-quadrotor system encircling a moving target (red full line).

To reflect the characteristics of formation clearly, we capture three fragments in Fig. 6, and it is easy to observe the formation variation in the hunting process. As is expected, the formation rotates asymptotically from large size to small, which makes the target in the center of the formation. The formation size $s(t)$ and the formation center $c(t)$ are the important indicators of the formation performance. One can see that the

error between formation's center and target $c(t)$ are shown in Fig. 7. The formation size $s(t)$ in Fig. 8 converges to the expectation asymptotically. In Fig. 9, the distortion of controller signals cancels out the effect of the disturbance, and the error of disturbance in Fig. 10 is bounded. The multi-quadrotor system has completed the hunting of the target, and we can adjust the formation scale by adjusting the value of d_i. Thus it can be seen that the simulation illustrates the effectiveness of the proposed protocols.

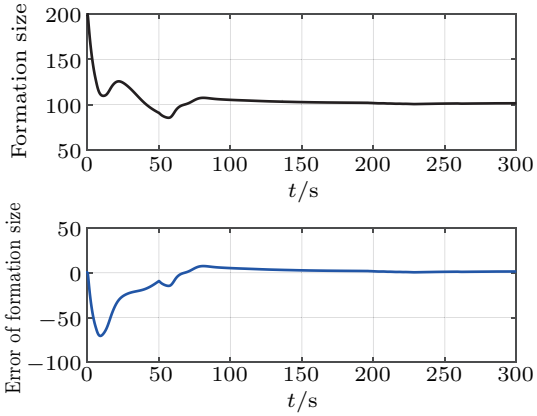


Fig. 7. (a) The size of the formation and (b) its error.

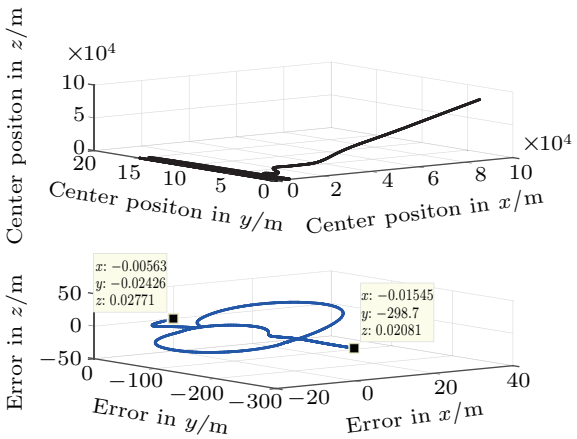


Fig. 8. (a) The center position of the formation and (b) its error.

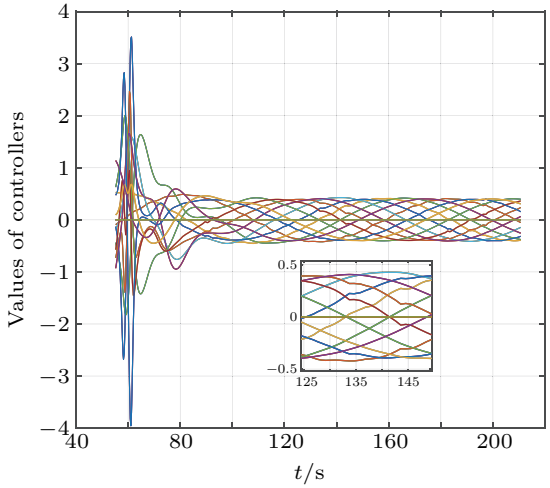


Fig. 9. The controller outputs values of all the quadrotors.

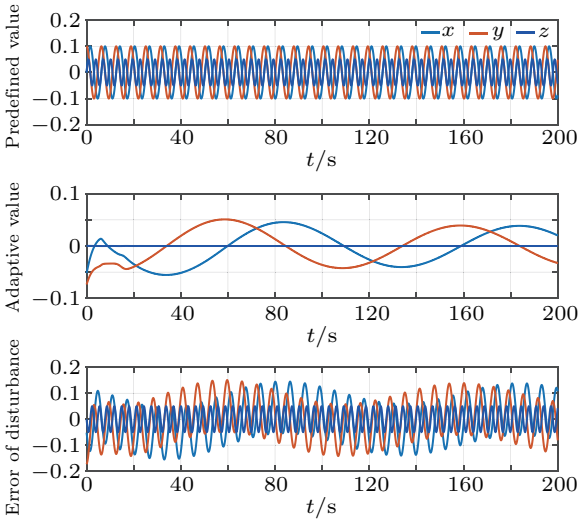


Fig. 10. The values of disturbance in the quadrotor 1 in x (Cambridge blue), y (red) and z (dark blue) directions.

7. Conclusion

We have studied the bearing hunting protocols in a multi-quadrotor system. First, we have modeled the machine vision for obtaining the bearing state among the quadrotors and target. In the process of controller design, we have achieved the collision avoidance of the quadrotors system through hybrid displacement control. Considering the limits of the transmission capability of the data link, we have adopted the hierarchical network based on bearing constraints to reduce the information needed in formation maintenance. We have given some simulations to illustrate the effectiveness of the proposed protocol.

One area for future research is taking event-triggered and sampling communication into account in the hunting process.

References

[1] Liu S and Hu L 2019 *Proc. 12th International Conference on Intelligent Robotics and Applications*, August 8–11, 2019, Shenyang, China, p. 267

[2] Hua Y Z, Dong X W, Hu G Q, Li Q D and Ren Z 2019 *IEEE Trans. Automat. Control.* **64** 4292

[3] Wang X H, Chen Z Q and Yuan Z Z 2015 *J. Franklin Institute* **352** 5437

[4] Gao M X, Xu X W, Klinger Y, Woerd J and Tapponnier P 2017 *Sci. Rep.* **7** 8281

[5] Pang S K, Wang J, Liu J Y and Yi H 2018 *Proceedings of the Institution of Mechanical Engineers, Part I: Journal of Systems and Control Engineering* **232** 819

[6] Roy D, Chowdhury A, Maitra M and Bhattacharya S 2018 *IEEE/RSJ International Conference on Intelligent Robots and Systems (IROS)* October 1–5, 2018, Madrid, Spain, pp. 4854–4861

[7] Liu X Z, Zhang K X and Xie W C 2018 *Nonlinear Anal-Hybri.* **30** 134

[8] Zou W C and Xiang Z R 2018 *IEEE Trans. Systems, Man, and Cybernetics: Systems* **49** 2478

[9] Min H F, Xu S Y, Li Y M, Chu Y M, Wei Y L and Zhang Z Q 2018 *J. Franklin Institute* **355** 2645

[10] Oh K K, Park M C and Ahn H S 2015 *Automatica* **53** 424

[11] Wu Z X, Sun J S and Wang X M 2018 *Chin. Phys. B* **27** 060202

[12] Tron R, Thomas J, Loianno G, Daniilidis K and Kumar V 2016 *IEEE Contr. Syst. Mag.* **36** 44

[13] Eren T 2011 *Eurasip J. Wirel. Commun.* **1** 72
[14] Zhao S Y and Zelazo D 2016 *IEEE Trans. Automat. Control.* **61** 1255
[15] Tran Q V, Park S H and Ahn H S 2018 *IEEE Conference on Control Technology and Applications (CCTA)*, August 21–24, Copenhagen, Denmark, pp. 658–663
[16] Zeng Z W 2017 *Multi-agent Coordination Control with Nonlinear Dynamics, Quantized Communication and Structure-constraint* (PhD Dissertation) (Changsha: National University of Defense Technology) (in Chinese)
[17] Li X L, Luo X Y, Wang J E, Zhu Y K and Guan X P 2018 *Neurocomputing* **306** 234
[18] Kim H, Lee D, Oh T, Lee S W, Choe Y and Myung H 2013 *Robot Intelligence Technology and Applications* **2** 3
[19] Liu J K 2015 *Sliding mode control design and MATLAB simulation: the design method of advanced control system* (Beijing: Tsinghua University Press) pp. 379–385
[20] Bouzid Y, Siguerdidjane H and Bestaoui Y 2018 *Proceedings of the Institution of Mechanical Engineers, Part I: Journal of Systems and Control Engineering* **232** 709
[21] Milford M J, Schill F, Corke P, Mahony R and Wyeth G 2011 *IEEE Int. Conf. Rob. Autom.* May 9–13, Shanghai, China, 2506
[22] Scaramuzza D and Fraundorfer F 2011 *IEEE Robot. Autom. Mag.* **18** 80
[23] Somasundaram G, Cherian A, Morellas V and Papanikolopoulos N 2014 *Comput. Vis. Image Und.* **123** 1
[24] Bai L, Chen F and Lan W Y 2015 *Chin. Phys. B* **24** 090206